

Hydroisomerization of C₆ with a zeolite membrane reactor

Leszek Gora*, Jacobus C. Jansen

Ceramic Membrane Centre, The Pore, DelftChemTech, Delft University of Technology, Julianalaan 136, 2628 BL Delft, The Netherlands

Received 18 July 2004; revised 19 October 2004; accepted 23 November 2004

Abstract

C₆ “once-through” hydroisomerization was investigated in a membrane reactor combining platinum containing chlorinated alumina fixed-bed catalyst and a silicalite-1/TiO₂/SS tubular membrane. In this application of a silicalite-1 zeolite membrane the feed mixture is passed over the membrane, where the linear molecules are separated and fed to the catalyst in the zeolite membrane reactor. The membrane reactor performance has been studied as a function of temperature and sweep gas flow rate. Separated *n*-C₆ from 2-MP (selectivity 24) is converted for 72%, with 36% selectivity for di-branched isomers (at 393 K, H₂ sweep 50 ml/min). The results indicate that the platinum-containing chlorinated alumina/silicalite-1 membrane reactor has a high potential for upgrading octane values.

© 2004 Elsevier Inc. All rights reserved.

Keywords: Membrane reactor; Silicalite-1 membrane; *n*-Hexane hydroisomerization; AT-2G catalyst

1. Introduction

Future demand for high-octane additives in gasoline will probably span decades. Compounds based on lead complexes and oxygen-containing components like MTBE and ETBE as well as aromatics are fading from the gasoline pool [1]. The production of high-octane branched alkanes based on the hydroisomerization of light paraffins, already in existence for a decade, will most likely continue. The state-of-the-art processes for hydroisomerization are based on separate catalyst and adsorber sections. The adsorption columns separate branched molecules from unconverted linear molecules that are transferred to the catalyst section in a recycle step. With the development of ceramic membranes based on zeolites [2], new opportunities emerge for a.o. equilibrium limited reactions. In isomerization reactions (e.g., to upgrade gasoline) a mixture of linear, mono-branched, and di-branched molecules are formed. However, because of thermodynamic equilibrium, the linear molecules cannot be fully converted to the desired di-branched molecules.

In an application of MFI zeolite the product mixture is passed over a membrane, where the linear molecules are separated and fed to the catalyst bed. Combining both sections in one unit either in a single pass or a recycle mode was first conceptually introduced by Krishna and Sie [3]. It is envisaged that higher efficiency, better process control, and lower consumption of energy might confer advantages over separate units. Moreover, the study might indicate the advantages and limitations to intensifying installations with respect to a whole class of reactions.

In a first approach to such an integrated system, a single pass of feed (*n*-hexane/iso-hexane) along the outside length of a tubular zeolite membrane was studied. *n*-Hexane permeates through the membrane and into the catalyst phase and is converted to iso-hexane. Products leave the reactor as isomers from the retentate and permeate sides of the membrane reactor (cf. Fig. 1). Improved mass and heat transfer properties are envisaged, as the distance between the separation and catalysis phase is minimized and the reactor unit runs isothermally.

In this paper we present the first part of a study on the hydroisomerization of C₆ in a single-pass operation with the use of a 30 cm² silicalite-1 membrane in a tubular configuration around a packed bed of Pt-chlorinated catalyst. The

* Corresponding author. Fax: +31 15 2784289.

E-mail addresses: L.Gora@tnw.tudelft.nl (L. Gora),
j.c.jansen@tnw.tudelft.nl (J.C. Jansen).

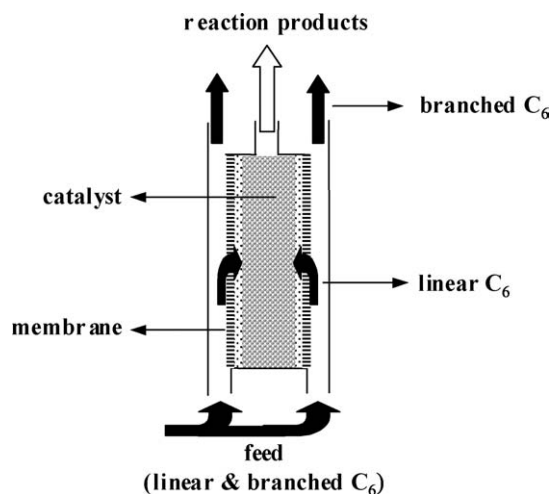


Fig. 1. Schematic drawing of a membrane reactor for hydroisomerization.

membrane reactor performance for C_6 hydroisomerization has been studied as a function of temperature and sweep gas flow rate.

2. Experimental

2.1. Membrane support

The support used in this work is composed of a sintered stainless-steel layer coated on the outside with a fine top TiO_2 layer. The TiO_2 layer was very smooth, with a mean pore size of about 100 nm (see Fig. 2a). Table 1 lists some physical characteristics of the support. Zeolite membranes were grown on the titania side of a Trumem [4] tubular porous support (10 mm outer diameter; Fig. 2b). The ends of the support were welded to nonporous metal tubes with a Swagelok connection (12 mm) on one side for mounting in the permeation testing equipment, and the other side of the tube was closed (dead end). The length of the porous part available for permeation was 10 cm, giving a total membrane surface of ca. 30 cm². No pretreatment or cleaning of the support was necessary before the synthesis.

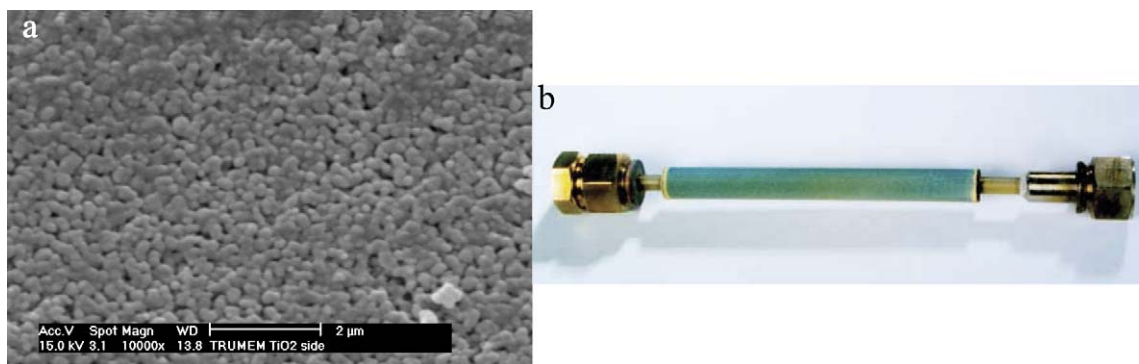


Fig. 2. Support material used in zeolite membrane synthesis. (a) TiO_2 side of the support. (b) Tubular silicalite-1 membrane with Swagelok connection on one side and dead end on the other.

Table 1
TrumemTM- TiO_2 -coated stainless-steel porous support^a

Layer	Thickness (μm)	Mean pore size (μm)	Porosity (%)
Stainless-steel	200	2–5	35
TiO_2	15	0.1	30

^a TrumemTM filters are made in Russia, by Trumem International [4].

2.2. Membrane preparation

The silicalite-1 membranes were prepared by two subsequent crystallizations under different conditions. The goal of the first synthesis, done at a low temperature (393 K, 114 h), was to enhance nucleation and to cover the support with a dense population of small crystals. The second synthesis was performed under conditions favoring fast crystal growth (453 K, 17 h) to enhance the closing of gaps between crystals in the layer. This synthesis strategy on a small scale with 25-mm-diameter disks had already been successfully applied in our laboratory [5]. The molar composition of the zeolite synthesis solution was 100 SiO_2 :59.3 TPABr:63.7 TPAOH:14200 H_2O . We prepared the zeolite synthesis solution by mixing tetrapropylammonium hydroxide (Chemische Fabriek Zaltbommel CFZ B.V., 25% in water), deionized water, and tetrapropylammonium bromide (CFZ B.V.). Tetraethylortho silicate (Aldrich) was used as the silica source. After TPABr was completely dissolved, silica was added to the solution. The initially turbid mixture was aged with stirring at room temperature until the solution became clear (6 h). From this solution, zeolite membranes were grown on the TiO_2 side of the tubular supports, which were placed vertically in the Teflon-lined autoclave. Each end of the tube, equipped with a Swagelok nut, was wrapped with Teflon tape and plugged with a Teflon cap. After the first synthesis the membrane was transferred into a new reactor, where a fresh precursor solution was used.

The final silicalite-1 membrane was washed several times with distilled water until any remaining synthesis reaction mixture was removed completely. The last two washings were done for 5 min in an ultrasonic bath. After the membrane was dried at room temperature overnight, it was cal-

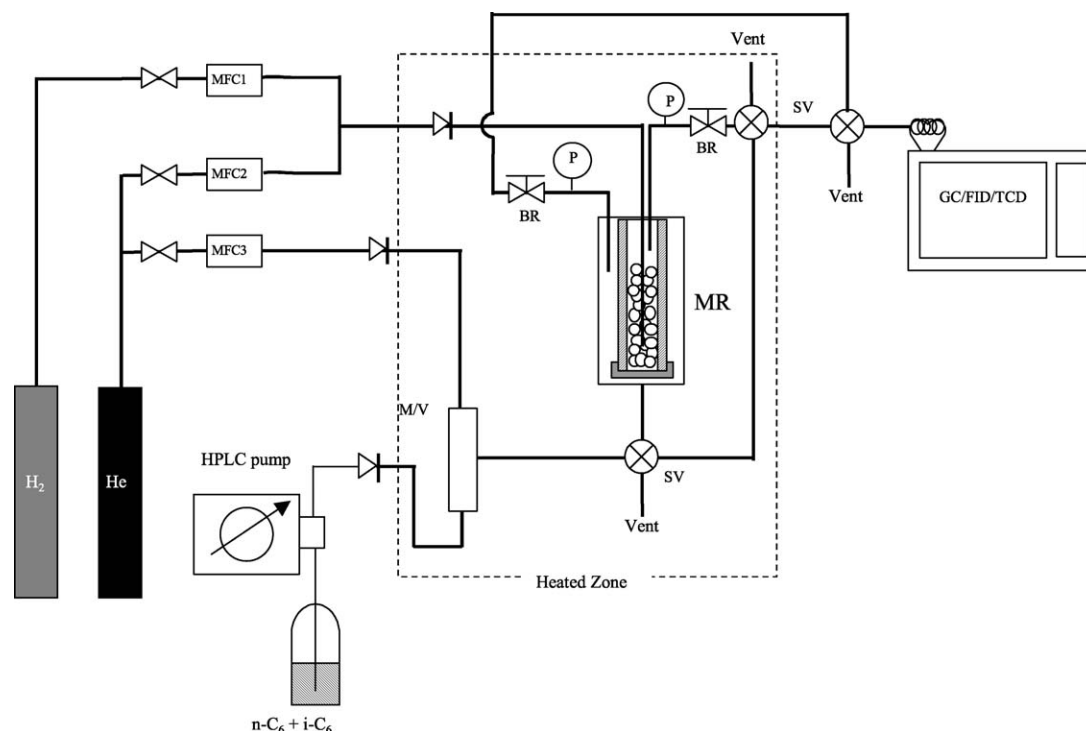


Fig. 3. Schematic diagram of the membrane reactor set-up. (MR) membrane reactor with packed catalyst bed, (MFC) mass flow controller, (M/V) feed mixer and vaporizer, (SV) selection valve, (P) pressure transducer, (BR) back pressure regulator, (GC/FID) gas chromatograph with flame ionization detector.

cined for 16 h in air at 673 K. Heating and cooling rates of 1 K/min were applied. The resulting membrane was analyzed for its potential use in the separation of linear from branched hydrocarbon. An Olympus BH2 optical microscope was used for the estimation of macroscopic integrity and the presence of cracks in the layer before and after calcination.

2.3. Apparatus and experimental procedure

The reactor setup, including the membrane in a hot-air oven and feed and carrier gas supply units, is shown in Fig. 3. Helium was used as a carrier gas at a flow rate of 50 ml/min to feed the shell side of the reactor with a mixture of hydrocarbons. A feed mixture of 80 wt% *n*-C₆ and 20 wt% 2-MP was supplied to the system via a HPLC pump. In different experiments either helium or hydrogen was used as a sweep gas. All gases and liquids supplied as a feed, carrier, or sweep were dried on line, with the use of molecular sieve 3A. Feed, retentate, and permeate streams were analyzed with a gas chromatograph (HP5890 series II with CP-Sil Pona CB column, FID detector for the hydrocarbon measurements). Before C₆ permeation experiments, we characterized the membrane by measuring the permeation of binary mixtures of *n*/*i*-butane at atmospheric pressure and 303 K introduced to the feed via mass flow controllers. The total pressure of 1 bar on both sides of the membrane was equal (Wicke–Kallenbach method). Helium was used as a sweep gas at a flow rate of 100 ml/min. The selectivity obtained was used to indicate the membrane quality.

Two sets of experiments were carried out to examine the performance of the catalytic membrane reactor. The first set of experiments was carried out without catalyst and was used to characterize the permeation properties (selectivities, fluxes) of the feed components through the membrane. The measurements were made between 353 and 413 K, for helium sweeping flow rates from 5 to 200 ml/min STP. In the second set of experiments we analyzed the combined separation and catalytic features of the membrane reactor by filling the membrane tube (volume $7.46 \times 10^{-6} \text{ m}^3$) with 5.19 g of platinum on chlorinated alumina catalyst particles (AT-2G) ($6.96 \times 10^5 \text{ g}_{\text{cat}}/\text{m}^3_{\text{reactor}}$) (supplied by Akzo Nobel) under dry conditions. The effects of temperature and sweeping flow rate on the performance of the membrane reactor were investigated as well.

3. Results and discussion

3.1. Membrane synthesis and evaluation

In a typical zeolite membrane synthesis, crystallization takes place on the support and in the reaction mixture. The difficulty with such syntheses is to force nucleation only on the support and continuous crystal growth from those nuclei toward a closed layer. In the case of a horizontally oriented support, the zeolite layer can form simply as a result of deposition of colloidal or submicrometer crystals from a bulk solution onto the support surface [6,7]. When the support is vertically oriented in the reaction mixture, a layer cannot

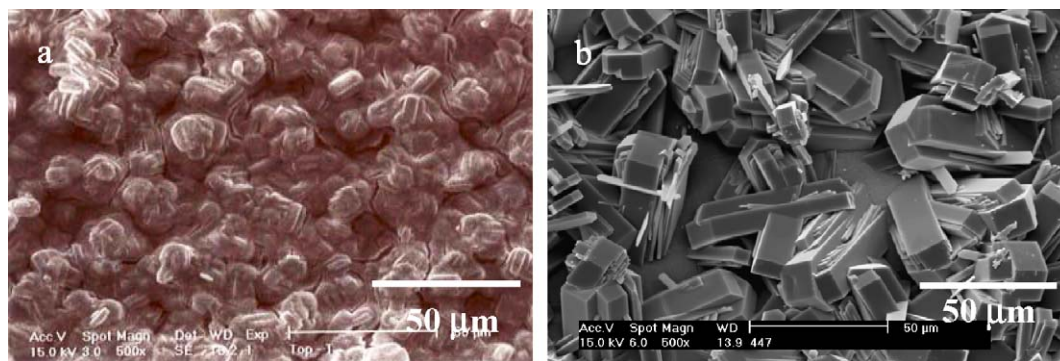


Fig. 4. SEM photographs of silicalite-1 synthesized on the vertically oriented support at (a) 393 K for 114 h; (b) 453 K for 17 h.

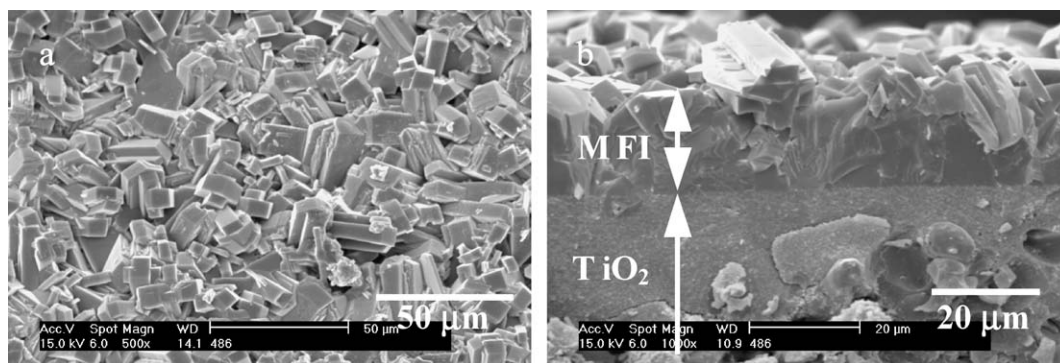


Fig. 5. SEM photographs of silicalite-1 synthesized on the vertically oriented support in two subsequent synthesis; 393 K for 114 h followed by 453 K for 17 h. (a) Top view; (b) cross-section.

form because of crystal settlement, but the nucleation has to take place on the surface of the support. In such cases seeding is a common solution for enhancing coverage of the support with crystals [8–11]. In our zeolite membrane synthesis we used a different method of increasing the nucleation rate on the support material. It is known that temperature is an important synthesis parameter that controls both the number of crystals nucleated and the rate of crystal growth. The number of nuclei decreases and the crystal growth rate increases as the synthesis temperature increases [12,13]. When the nucleation and crystal growth processes are separated and performed under different conditions, the synthesis is better controlled and results in a better membrane. After the nucleation stage, an elevated temperature can be used to accelerate the crystal growth to form a closed layer.

Single synthesis performed on a vertically oriented support at either 393 K for 114 h or 453 K for 17 h does not result in formation of a closed zeolite layer. Figs. 4a and 4b show top views of supports after syntheses at 393 K for 114 h and 453 K for 17 h, respectively. It is clear that with decreasing crystallization temperature the support is covered by a larger number of small crystals. The high-quality silicalite-1 membrane (Fig. 5) is formed when the second synthesis at 453 K for 17 h is performed on a sample synthesized previously at 393 K for 114 h. The membrane was about 15 µm thick.

This two-stage synthesis is successfully applied for silicalite-1 synthesis on a vertically oriented tube (~30 cm² surface area). In view of the limited literature data on the up-scaling of zeolite membrane preparations and of the recent advances in reproducible syntheses of high-quality silicalite-1 membranes in our laboratory [6], we developed “in-house” techniques for synthesizing up-scaled tubular membranes. The thickness of the zeolite membrane synthesized on a vertically oriented tubular support is uniform along the length of the membrane. The tubular support, with a surface area of 30 cm², is quite large compared with most zeolite membranes reported in the literature, which are usually less than 5 cm². The largest MFI-type membrane reported in the literature has a surface area of 60 cm² and shows permselectivity for H₂/SF₆ = 35 [14]. Unfortunately, the authors did not report *n/i*-butane selectivity; therefore, it is difficult to compare this membrane performance with those of other membranes. The *n/i*-butane mixture selectivity is generally used as a measure of membrane quality by several investigators [11,15–19].

Before C₆ permeation experiments the synthesized tubular membrane of the current study was characterized by permeation measurements of binary mixtures of *n/i*-butane at 303 K. A 40:60 *n/i*-butane feed mixture was used. At 303 K, the mixture selectivity of *n/i*-butane was as high as 45.3. The high selectivity is accompanied by reasonable fluxes. Table 2 compares data for the separation of butane

Table 2
Comparison of reported permeation results for 50:50 *n*/*i*-butane mixtures through MFI-type zeolite membranes at room temperature

Membrane/support with pore size	Thickness (μm)	Size	Conditions	<i>n</i> -Butane flux ($\text{mmol}/(\text{m}^2 \text{ s})$)	Selectivity	Reference
ZSM-5/ α - Al_2O_3 $\sim 2 \mu\text{m}$	7	250 mm long 12 mm OD	303, WK	1.2	42	[15]
Silicalite/ α - Al_2O_3 top layer 100 nm	0.5	Disk 25 mm	298, WK	98	9	[16]
Silicalite/ α - Al_2O_3 top layer 135–165 nm	3	Disk 39 mm	298, WK	0.83	52	[17]
Silicalite/ TiO_2 /SS top layer 100 nm	30	Disk 25 mm	303, WK	3.24	28	[2]
Silicalite/ TiO_2 /SS top layer 100 nm	35	Disk 25 mm	303, WK	2.75	55	[18]
Silicalite/ α - Al_2O_3 150 nm	1–30	Disk 22 mm	295, WK	1–4	30–70	[11]
Silicalite/ α - Al_2O_3 150 nm	Inside support 100 μm	50 mm long 10 mm OD	298, WK	3	4.5	[19]
Silicalite/ TiO_2 /SS top layer 100 nm	15	100 mm long 10 mm OD	303, WK	5.64	45.3 ^a	This work

^a 40:60 *n*/*i*-butane mixture.

mixtures obtained here with the literature data. The membrane size and thickness are also given in Table 2. There is no clear correlation between the membrane thickness and the fluxes of the permeating hydrocarbons. The thinnest membrane (500 nm) gives a very high flux with relatively low selectivity. The membranes reported in the literature were prepared by different methods. Therefore, morphologies of the membranes may differ. As a result, membranes with similar thicknesses may perform quite differently. Some differences may also be due to different conditions used for testing, such as total pressure (120 kPa [15], 101 kPa [16,17]), the sweep gas used (Ar [15], He [16,17], N_2 [19]), and temperature (295 K [11,16,17,19], 303 K [2,15,18]). It is well known that separation of butane isomers at low temperature is governed by the surface diffusion mechanism [2], which is strongly influenced by experimental conditions [20]. The high *n*/*i*-butane selectivity of our membrane (45.3) indicates that the membrane is of very high quality compared with those reported in the literature. This is especially true because a feed enriched in *i*-butane was used (40:60 compared to 50:50 *n*-butane/*i*-butane). Recently Nishiyama reported [2] that permeation of butane isomer mixtures at low temperatures is strongly affected by the feed composition and the feed pressure of the butane mixture. Mixtures with higher molar ratios of *n*-butane to *i*-butane lead to higher selectivities [2]. Pore blocking by *n*-butane increases with increasing partial pressure of *n*-butane, and, consequently, the selectivity for *n*-butane is improved.

3.2. *n*-Hexane/2-methyl-pentane separation

After analyzing our silicalite-1 membrane and obtaining a high selectivity for butane isomers, we investigated further the potential of this membrane for separating linear from

branched C_6 alkanes. The C_6 isomer mixture is of particular interest because its components are important constituents of gasoline. According to Krishna et al. [21] the separation selectivity of hydrocarbon isomers through silicalite-1 zeolite membranes is the product of S_{MS} , the ratio of the corrected diffusivities of the components, and S_{T} , the thermodynamic selectivity factor. The corrected diffusivity depends on the size of the permeant and the size of the windows or apertures in zeolites used and on the strength of the host-adsorptive interactions. The diffusivity generally increases with an increase in the size of the diffusion pathway. The thermodynamic selectivity factor S_{T} is strongly related to the strength of the host-adsorptive interactions. At very low occupancies, that is, in the Henry's law regime, S_{T} is equal to the ratio of the adsorption equilibrium constants of the components. The adsorption equilibrium depends on how well each molecule can adjust its shape to fit the silicalite-1 channel network and on how strongly it interacts with the framework. The *n*-hexane molecule is sufficiently flexible; therefore it is easily accommodated in the region of low potential energy close to the channel wall. For molecules with more branches in the alkane chain, only some of the centers can sit in the low-energy regions, whereas other centers are forced to occupy less energetically favorable positions further from the wall. This means that the high sorption selectivity for the linear alkane is due to entropic effects; the linear alkane has a higher "packing" efficiency than the branched alkane within the zeolite structure. For the same reasons, it is easier to separate *n*-hexane from double-branched than from single-branched isomers.

According to Zhu et al. [22], 2-methyl-pentane (2-MP) and 3-methyl-pentane (3-MP) show very similar adsorption behaviors under the same conditions, but the diffusivity of

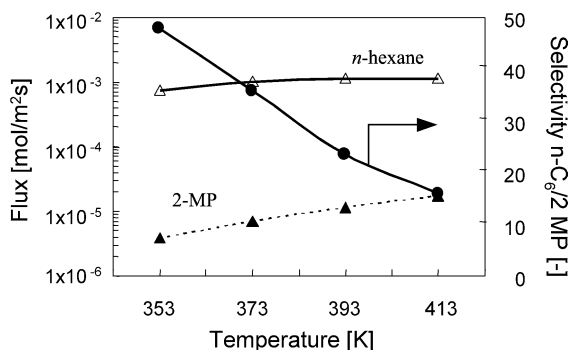


Fig. 6. Fluxes and selectivity for 80:20 *n*-hexane/2-MP through a silicalite-1 membrane as a function of temperature.

2-MP is almost twice as high as that of 3-MP. The longer tail in the 2-MP molecules provides a somewhat more favorable orientation for the molecule through the silicalite-1 channels compared with 3-MP. Therefore, the most difficult separation in binary mixtures of *n*-hexane from its isomers seems to be for an *n*-hexane/2-MP mixture. It is well established in the literature that at low temperatures *n*-hexane (kinetic diameter 4.3 Å) adsorbs selectively in MFI from mixtures with its isomers 2-MP and 3-MP (kinetic diameter 5 Å), 2,2-dimethyl-butane (2,2-DMB), and 2,3-dimethyl-butane (2,3-DMB) (kinetic diameter 6.2 Å). Selective adsorption is dependent on the temperature, feed composition, and Si/Al ratio in the membrane. At higher temperatures the selectivity between *n*-hexane and 2-MP in a binary mixture is attributed to the higher diffusivity of *n*-hexane compared with that of 2-MP.

The separation performance of our silicalite-1 membrane was investigated before the isomerization reaction with the membrane reactor. Separations of 80:20 *n*-hexane/2-MP feed mixtures were measured as a function of temperature through our silicalite-1 membrane. Helium flow at 50 ml/min was used as a sweep gas and as a carrier gas. The molar composition of the feed was 77.67% helium, 17.86% *n*-hexane, and 4.47% 2-MP.

Fig. 6 shows the fluxes and the permeation selectivities (*n*-hexane/2-MP) as a function of temperature. Normal hexane permeates significantly faster than 2-MP. The flux of *n*-hexane is a weak function of temperature and is approximately 1 mmol/(m² s) over the temperature range of 353–413 K. A similar trend has been reported in the literature [23]. The weak temperature dependence of the flux gives more freedom when it comes to selecting the conditions at which the hydroisomerization reaction will be run. With increasing temperature, the permeance difference between *n*-hexane and 2-MP decreases, and therefore the selectivity decreases as well. The maximum selectivity was measured at the lowest temperature (353 K) studied; it was equal to 48. The separation selectivity of 24 between *n*-hexane and 2-MP at 393 K is still reasonably high. Normal hexane adsorbs more strongly than 2-MP at low temperature and thus blocks zeolite pores for 2-MP. These differences in interactions of *n*-hexane and 2-MP with the zeolite resulted in selectivity

for *n*-hexane. With increasing temperature the adsorption selectivity for *n*-hexane becomes less dominant, resulting in a decrease in *n*-C₆/2-MP selectivity. The contributions by adsorption and diffusion govern the permeation selectivity of alkanes through silicalite-1 membranes. The diffusion differences between individual components dominate the selectivity at high temperatures.

Recently Schuring et al. [24] used radioactively labeled molecules to measure self-diffusivity of *n*-hexane and 2-MP molecules in binary mixtures at 433 K in MFI crystals. For an 80:20 *n*-hexane/2-MP feed, the self-diffusivity of *n*-hexane was about 6 times higher than the diffusivity of 2-MP. The *n*-hexane/2-MP selectivity studied here at the highest temperature (413 K) for the same feed composition (80:20 *n*-hexane/2-MP) was equal to 18. Higher selectivity is expected at lower temperatures (413 K instead 433 K). However, the higher total hydrocarbon pressure of 22 kPa in our studies, compared with 6.6 kPa in Schuring's measurements (with the same feed composition), could also enhance the *n*-hexane/2-MP selectivity. At low hydrocarbon loadings, the *n*-C₆ locates within the channels, and branched alkanes locate at the MFI intersections. According to Krishna et al. [21] there is an increase in adsorption selectivity beyond a total loading of four molecules per unit cell, corresponding to a situation in which all of the intersections are occupied (above a pressure of 15 kPa). Because of a configurational entropy effect, an increase in the mixture loading above four molecules per unit cell causes normal alkane molecules to replace branched molecules within the zeolite structure.

Most of the literature data on the separation of hexane isomers deals with the separation of *n*-hexane and double-branched isomers. The selectivities obtained are between 17 and 1000, depending on the quality of the membranes and the experimental conditions. However, far fewer data on *n*-hexane/2-MP separation are available. The *n*-hexane/2-MP selectivities measured in this study are comparable to the available literature data. Experimental values of the selectivity obtained by Funke et al. [25] for a 50/50 mixture of *n*-C₆ and 3-MP through silicalite-1 also showed that the selectivity decreased with increasing temperature: from 24 at 326 K to 1.1 at 443 K. Matsufuji et al. [26] performed pervaporation at the separation of *n*-hexane/2-MP mixtures with a ZSM-5 membrane at 303 K. For the 50/50 *n*-hexane/2-MP mixture, the selectivity was 54. Similar *n*-hexane/3-MP selectivity ranging between 50 and 75 at 373 K was reported by Flanders et al. [23]. Direct comparison of our results with the fluxes published in the literature is very difficult because of a lack of data and because of differences in the operating conditions. In Tables 3 and 4 we summarize the available literature data and point out differences in experimental conditions.

The single component fluxes of *n*-hexane through MFI membranes reported in the literature are around 1 mmol/(m² s) (at about 373 K) and are comparable to our results. In addition to differences in the membrane quality, some diver-

Table 3
Comparison of reported *n*-hexane fluxes in single component permeation measurements through MFI membranes

Zeolite/support	Membrane thickness (μm)	Surface area (cm ²)	Feed <i>n</i> -C ₆ pressure (bar)	Temperature (K)	Flux (mmol/(m ² s))	Reference
Sil-1/100 nm TiO ₂	18	31.4	0.18	373	1.1	This work
ZSM-5/5 nm γ-Al	2–10	5.5	0.3	383	2.25	[25]
ZSM-5/5 nm γ-Al	25–30	5.5	0.18	373	1.15	[27]
ZSM-5/5 nm γ-Al			0.05	374	1.298	[28]
ZSM-5/5 nm α-Al	20	4.4	0.13	373	1.45	[29]
ZSM-5/500 nm SS	25–30		0.07	373	0.966	[23]
Sil-1/100 nm α-Al		0.5	Pervaporation	303	0.022	[26]

Table 4
Comparison of reported *n*-hexane fluxes in binary permeation through MFI membrane

Zeolite/support	Membrane thickness (μm)	Surface area (cm ²)	Feed pressure (bar)		Temperature (K)	Flux (mmol/(m ² s))		Separation selectivity <i>n</i> -C ₆ /2- or 3-MP (–)	Reference
			<i>n</i> -C ₆	2-MP		<i>n</i> -C ₆	2- or 3-MP		
Sil-1/100 nm TiO ₂	18	31.4	0.18	0.005	373	1.02 0.0068 ^a	–	38	This work
ZSM-5/100 nm α-Al	0.5	2.83	0.13	–	373	7.02	–	–	[16]
ZSM-5/5 nm γ-Al	2–10	5.5	0.18	0.18	362	0.83 0.0345 ^b	–	24	[25]
ZSM-5/500 nm SS	25–30		0.07	0.07	373	0.348 0.0068 ^b	–	50	[23]
Sil-1/100 nm α-Al	20	0.5	Pervaporation		303	0.013 4 × 10 ^{−4a}	–	54	[26]

^a 2-MP.

^b 3-MP.

sity in measured fluxes can be due to disparities in support porosities. The effective membrane area is not the same as the support surface area because the support partially blocks the membrane. The highest *n*-C₆ flux of 2.25 mmol/(m² s) was reported by Funke et al. [25]. However, this flux was measured at a temperature 10 K higher, and the driving force was also the highest compared with the others (0.3 bar pressure of *n*-hexane).

There is no clear relation between the membrane thickness and the fluxes based on the literature data. A very high flux of *n*-C₆ in binary *n*-C₆/2,2-DMB mixture permeation was reported for a thin 0.5-μm membrane by Hedlund et al. Unfortunately, the selectivity of *n*-C₆/2-MP was not investigated for that membrane. Matsufuji et al. [26] published permeation results for *n*-C₆ in a binary mixture with 2-MP, but unfortunately only for a pervaporation configuration. The driving force in pervaporation, as the surface of MFI membrane is most likely saturated, is high. It may be comparable to the driving force in vapor permeation when the adsorption of hexane isomers at the feed side is saturated. On the other hand, the diffusivity of *n*-C₆ in MFI at 303 K (pervaporation) is lower than that at 373 K (vapor permeation). Consequently, a much lower *n*-C₆ flux in pervaporation [26] was measured, compared with our vapor permeation *n*-C₆ flux value. The other two sources report lower fluxes of *n*-C₆ comparable to our results. The selectivity of *n*-C₆/3-MP measured by Flanders et al. [23] was 50. As was pointed out earlier, because of more favorable fitting of 2-MP compared with 3-MP inside MFI channels, it

is easier to separate 3-MP than 2-MP from a mixture with *n*-C₆ [22].

3.3. Sweep gas

In the membrane reactor the reactant permeation rates must match the catalytic conversion rate at the desired operating conditions. Accumulation of reactants or products on the catalyst must be avoided. Rapid sweeping of the permeate minimizes buildup of the reaction products in the catalyst and promotes more reaction. Applying a sweeping gas on the permeate side has been a proven method of increasing the driving force for membrane permeation [20]. Introducing a significant quantity of the carrier (or sweep) gas to the permeate side of the membrane, however, has two major implications. One is that it may create the need to separate the permeate (products) from the carrier gas downstream of the membrane reactor operation. The other is the cost associated with the sweep gas. The best scenario is one in which a component that is needed for the reaction taking place on the catalyst located on the permeation side can be simultaneously used as a sweep gas. In our studies, H₂ is needed for the hydroisomerization reaction. Therefore, in catalytic tests of our zeolite membrane reactor, hydrogen was used as a sweep gas. However, in the permeation tests the components permeating the silicalite-1 membrane were swept with helium instead of hydrogen for safety reasons.

As expected, the sweep gas flow rate was one of the important parameters influencing the permeation fluxes and the

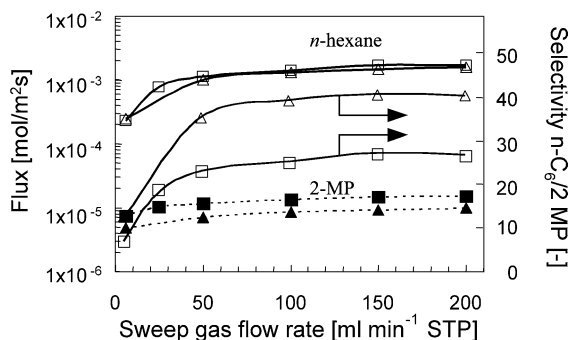


Fig. 7. Fluxes and selectivity for 80:20 *n*-hexane/2-MP through a silicalite-1 membrane as a function of the sweep gas flow rate. Δ , \blacktriangle —373 K; \square , \blacksquare —393 K.

selectivity. Fig. 7 shows the sweep gas flow rate effect on the fluxes of *n*-C₆ and 2-MP and the permeation selectivities (*n*-hexane/2-MP) in the permeation of the binary mixture from an 80:20 feed of *n*-C₆/2-MP at 373 and 393 K. The effects of the sweep gas flow rate on permeation at the two temperatures are similar. More efficient removal of the permeating components increases the fluxes. This effect is larger on the flux of *n*-C₆ than on 2-MP. This is explained by the fact that the adsorption equilibrium constant of *n*-C₆ is higher than that of 2-MP, so a change in the downstream partial pressure affects the coverage, and thus the driving force, of *n*-C₆ more than that of 2-MP. The higher driving force for *n*-C₆ than 2-MP gives a higher mobility of *n*-hexane in the zeolite pores and thus a higher selectivity. Especially at a low sweeping flow rate (below 50 ml/min), this influence is remarkable (see Fig. 7). At high sweep gas flow rates the permeate pressure on the zeolite/support interface is low, resulting in high concentration gradients across the zeolite, which are the driving force for permeation. Increasing the sweep gas flow rate beyond 50 ml/min has little effect on the fluxes and the selectivities because the permeate partial pressures at the zeolite/support interface are not further lowered under these conditions with increasing sweep flow rate. The support layer acts as a stagnant diffusion layer that is unaffected by a high flow rate. With decreasing sweep flow rate, permeating components are not removed as effectively and permeate partial pressures are higher. The fluxes of the components are significantly reduced by the fact that their permeate pressures are not equal to zero. In the mixture, the fastest component is the one most affected by the nonzero boundary conditions, since it has the highest concentration in the permeate. This reduces the selectivity of the membrane. The selectivities between *n*-C₆ and 2-MP are higher at lower temperature, as expected and explained earlier.

The increase in the flux of the permeating component with increasing sweep gas flow rate results in an increase in the permeation fraction (“membrane yield”). The permeation fraction is related to the flux and is defined as the fraction of the feed component that goes through the membrane:

$$\text{Perm.fraction}_i = \phi_{i,p} / \phi_{i,f}, \quad (1)$$

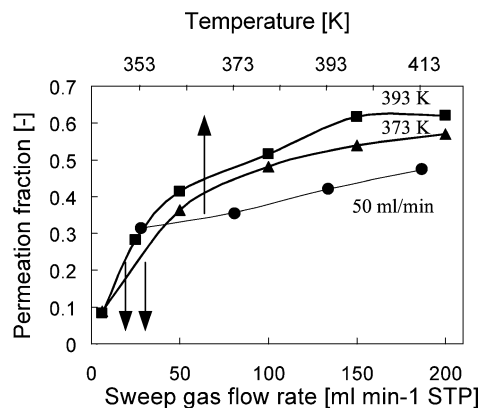


Fig. 8. Permeation fraction of *n*-C₆ for 80:20 feed mixture of *n*-hexane/2-MP through a silicalite-1 membrane as a function of temperature (at sweep gas flow rate 50 ml/min) and the sweep flow rate (at 373 and 393 K).

where $\phi_{i,p}$ and $\phi_{i,f}$ are molar flows of component *i* in the permeate (p) and feed (f), respectively.

Fig. 8 shows the effect of the sweep flow rate and temperature on the permeation fraction of *n*-C₆ at two temperatures, 373 and 393 K. The permeation fraction for the preferentially permeating component, which is *n*-C₆ in this case, can be as high as 0.6 at 393 K. This means that 60% of the *n*-C₆ feed goes to the permeating side under the applied conditions.

The effect of the temperature on the permeation fraction of *n*-C₆ was studied at a sweep flow rate of 50 ml/min. There is an increase in the permeation fraction with temperature up to 413 K.

3.4. Combined separation and reaction performance

Finally the combined separation and reaction in a “single-passage mode” were investigated as a function of temperature and sweep flow rate. The main objective of this part of the study was to show the feasibility of combining platinum-containing chlorinated alumina fixed-bed catalyst and a silicalite-1/TiO₂/SS tubular membrane (working at the same temperature). It is a basic requirement for making the process more productive and reducing operating costs.

The feed of 80:20 *n*-hexane/2-MP was used as a model study. Isomerization of *n*-hexane leads to four isomers, of which 2,3-DMB provides the highest octane number. According to the C₆ thermodynamic equilibrium, decreasing the hydroisomerization temperature favors the highly branched, high-octane alkanes. In addition, low temperatures favor the reduction of hydrocracking reactions. On the other hand, from a kinetic point of view, reaction rates are higher at elevated temperatures. Isomerization of *n*-hexane at low temperatures requires a very active catalyst to achieve a high enough production rate. Therefore, a compromise between the catalyst activity and the best C₆ thermodynamic equilibrium must be found.

The tube was filled with an AT-2G catalyst in a glove box under a N₂ atmosphere. These conditions were required

Table 5
Effect of replacing He with H₂ as a sweep gas on the membrane performance in 80:20 *n*-C₆/2-MP mixture separation at 393 K

Sweep gas at 50 ml/min	<i>n</i> -Hexane flux (mmol/(m ² s))	Selectivity
He	1.31	23.75
H ₂	1.12	28.15

because the catalyst is very sensitive to moisture, as 1.5–2.0 kg water destroys 100 kg of catalyst. Moisture traps in the feed lines to the reactor were another requirement for avoiding deactivation of the catalyst. It is expected that in the membrane configuration, according to the concept shown in Fig. 1, the catalyst will be protected from water and other possible contaminants contained in the feed by the hydrophobic silicalite-1 membrane.

A stable AT-2G catalyst operation is possible under hydrogen pressure. Therefore, He sweep gas previously used for membrane testing was replaced with H₂. The effect of replacing He with H₂ as the sweep gas on the membrane performance in *n*-C₆/2-MP separation is shown in Table 5. Our studies indicate that the use of H₂ instead of He as a sweep gas slightly influences fluxes and selectivities, the hydrocarbon fluxes decrease, and *n*-C₆/2-MP selectivity improves a little. Helium is always used as a carrier gas for the hydrocarbon feed. Since helium and hydrogen adsorb very weakly on silicalite-1 at the studied temperature range (353–413 K) [2], the effect of the counter-diffusion on the flux should be negligible. The hydrocarbons are expected to adsorb and effectively block He and H₂ from entering the zeolite channels. When He was used as a sweep gas there was no significant He partial pressure difference over the membrane because He was also used as a carrier gas. However, when He was replaced with H₂, the difference in its partial pressure across the membrane increased significantly. As a result the permeated hydrocarbons could be slightly suppressed by H₂ counter-diffusion, resulting in a decrease in the hydrocarbon fluxes through the membrane, especially at the membrane defect sides, where probably most of 2-MP permeates, resulting in improved *n*-C₆/2-MP selectivity.

An experiment performed with a nonactive catalyst (deactivated by exposure to moist air) showed that the presence of the catalyst did not influence the membrane properties. The measured fluxes and the selectivities for the binary 80:20 *n*-C₆/2-MP mixture were the same with and without the presence of a nonactive catalyst.

Table 6
Distribution of hexanes in the permeate, isomerized product in the membrane reactor as a function of temperature. The feed was 80:20 mixture of *n*-C₆/2-MP. H₂ sweep gas 50 ml/min

Temperature (K)	WHSV (g _{HC} /(g _{cat} h))	H ₂ /HC	% Distribution (molar)						<i>n</i> -C ₆ conversion (%)
			< C ₆	2,2-DMB	2,3-DMB	2-MP	3-MP	<i>n</i> -C ₆	
353	0.13	14.96	0.00	2.72	5.30	15.19	7.24	69.56	29.36
373	0.18	11.12	0.01	5.45	7.93	22.62	11.29	52.70	40.5
393	0.21	9.76	0.01	15.54	10.60	30.63	16.03	26.63	71.75
413	0.21	9.06	0.88	10.64	10.04	30.23	16.32	31.88	68.70

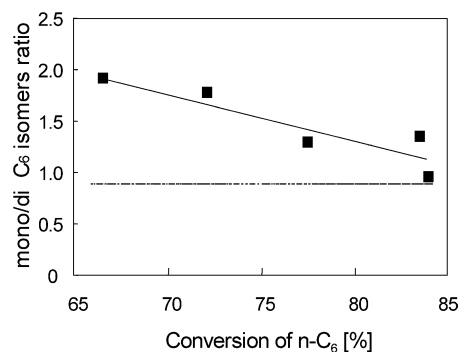


Fig. 9. The ratio of mono/di-branched isomers as a function of *n*-C₆ conversion on the permeate side of the membrane reactor. Based on % distribution of products on the permeate side, data from Tables 6 and 7.

The results of experiments carried out at different temperatures (with an active catalyst) are shown in Table 6. All data in Table 6 concern the permeate side of the membrane reactor. The sweep flow rate was maintained at 50 ml/min STP. The cracking reaction was negligible, especially at low temperatures; with increasing temperature there was a slight increase in the formation of components lower than C₆.

The reaction rate of the decomposition (cracking reactions) increased with increasing reaction temperature. Raising the temperature to 393 K resulted in an increase in the conversion to 71.75%, with a shift in the product distribution toward the double-branched components. As shown in Fig. 9, the ratio of mono/di-branched isomers depends strongly on the conversion and approaches the equilibrium value of 0.89. Temperature was not the only parameter that changed during these experiments. The H₂/HC ratios and weight hourly space velocity (WHSV) changed as well. The permeation rate of *n*-C₆ through the membrane increased slightly with increasing temperature (see Fig. 6). Because the H₂ sweep flow rate was constant, the molar ratio of H₂/HC decreased slightly. In addition, the WHSV increased as a result of the increased *n*-C₆ permeation.

Commercial units operate at a molar ratio of H₂/C₅-C₆ = 0.1, WHSV = 2 (g_{C₅-C₆}/(g_{cat} h)) and pressures of 25–30 bars. The H₂/*n*-C₆ ratios in our experiments are higher than 5. A higher content of H₂ is expected to protect the catalyst and prolong its lifetime by decreasing the coke deposition. The ratio between the conversion to iso-alkanes and the total conversion is a function of the reaction pressure and goes through a maximum at total pressures of 25 to 30 bars. Because of experimental restrictions, we had to run the hy-

Table 7

Distribution of hexanes in the permeate, isomerized product in the membrane reactor as a function of the sweep flow rate at 393 K. The feed was on 80:20 mixture of *n*-C₆/2-MP

H ₂ sweep (ml/min)	WHSV (gHC/(g _{cat} h))	H ₂ /HC	% Distribution (molar)						<i>n</i> -C ₆ conversion (%)
			< C ₆	2,2-DMB	2,3-DMB	2-MP	3-MP	<i>n</i> -C ₆	
6	0.04	5.59	8.5	34.6	6.2	25.6	13.7	11.3	83.6
25	0.14	7.15	1.3	24.6	10.5	30.0	15.7	17.8	77.14
50	0.21	9.76	0.01	15.54	10.6	30.63	16.03	26.63	71.75
200	0.31	26.06	0.00	1.1	2.7	8.2	4.1	83.8	24.38

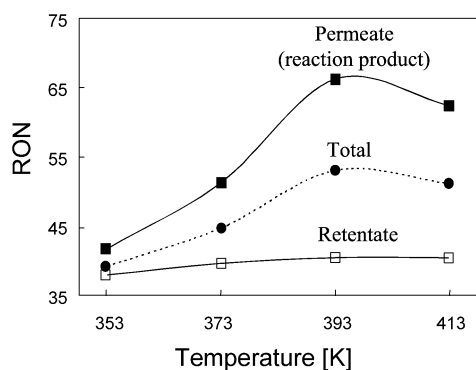


Fig. 10. The zeolite membrane reactor products RON number as a function of temperature. H₂ sweep gas 50 ml/min STP.

droisomerization reaction at 1 bar. It is expected that at 1 bar the catalyst performance is not optimal.

The effect of the sweep flow rate on *n*-hexane/2-MP conversion was investigated at 393 K, as shown in Table 7. In all studied cases the partial pressure of the feed of 80:20 *n*-C₆/2-MP was 22 kPa. The *n*-C₆ conversions decreased from 83.6 to 24.38% when the H₂ sweep flow rates were increased from 6 to 200 cm³/min STP. This decrease in conversion can be attributed to the shorter residence time of the *n*-hexane with increasing sweep flow rate.

The feed in the membrane reactor (see Fig. 1) was well distributed along the total length of the membrane. Based on the permeation data, the molar ratio of the H₂/HC mixture inside the reactor was between 5.5 and 26, and the space velocity had values up to 0.31 g_{feed}/(g_{cat} h). For commercial use in trickle flow-bed reactors, the conversion is highest (80–90%) at a WHSV of 2, which is higher by a factor of 10 than the one used here. With a lower WHSV (see Table 7), the AT-2G catalyst operates closer to the thermodynamic equilibrium for the isomerization reaction at a given temperature.

The research octane numbers (RONs) for permeate (reaction product) and retentate were calculated based on the stream compositions (see Tables 6 and 7). Fig. 10 shows the RON numbers as a function of the temperature. The permeate (reaction product) RON number reaches a maximum at 393 K. The position of this maximum is a consequence of complex dependences on separation selectivities and permeation fractions of *n*-C₆ and the compromise between the activity of the catalyst and the best thermodynamic equilibrium. The RON of the retentate stream increases slightly

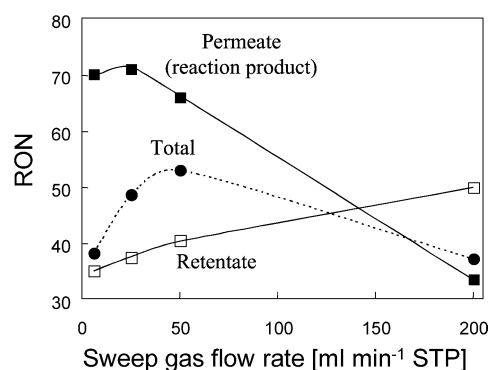


Fig. 11. The zeolite membrane reactor products RON number as a function of the sweep H₂ flow rate at 393 K.

with elevating temperature. This is a result of enriching the retentate with branched alkanes (2-MP) due to *n*-C₆ permeation through the membrane. The effect of the sweep gas flow rate on the RON of the permeate and retentate streams is shown in Fig. 11.

The highest total RON number (retentate + reaction product) was obtained for a H₂ sweep flow rate of 50 ml/min STP. The retentate RON increase reflects the permeation fraction of *n*-C₆ increase as a function of the H₂ sweep flow rate. At the same time, on the permeate side of the membrane, the WHSV increase causes the *n*-C₆ conversion to be low and the reaction products to shift far from the thermodynamic equilibrium.

The results for the “single-passage mode” reported in this paper form only a part of the complete study on the feasibility of the membrane reactor. In principle this is not the most suitable mode, because in “recycle mode” the retentate stream always has a higher RON number than the reaction side, since it is being purified from linear components. Therefore, the advantage of membrane reactor configuration for hydroisomerization should then become even clearer. However, the combined product (retentate + reaction product) from the membrane reactor in “single-passage mode” at 393 K and the H₂ sweep flow rate of 50 ml/min STP already gave a RON value about 3 points higher compared with values determined from the literature data on *n*-hexane hydroisomerization in a fixed-bed reactor for Pt-loaded zeolite beta and mordenite catalyst at similar *n*-C₆ conversion [30,31]. The RON was improved by 14 points by the use of a combined stream of reaction product and retentate over the RON of the feed.

In contrast to the feed used in this work, industrial feed streams (RONs of around 70) contain substantial amounts of *i*-C₅ and *i*-C₆ components. Since the membrane has shown reasonable selectivity, a higher retentate RON can be expected when industrial feed is used.

3.5. Remarks

The current industrial C₆ hydroisomerization process requires the separation and subsequent recycling of normal, unconverted hydrocarbons. With the zeolite membrane configuration shown in Fig. 1, there is no recycling of unconverted components. However, in continuation of these studies, a recycle mode will be studied as well.

The permeate RON depends on catalytic conversion of linear to branched hydrocarbons. Lower temperatures favor products with higher RONs. Because of equilibrium limitations, however, linear hydrocarbons will always be present in the product on the permeate side. To minimize the concentration of linear hydrocarbons in the permeate product, it may be necessary to recycle the permeate products. The more pure *n*-C₆ there are that permeate toward the catalyst, the higher the RON of the retentate will be. If the feed contains low amounts of normal hydrocarbons, then it could be difficult to accomplish the above goal with a silicalite-1 membrane. Therefore, the effect of the *n*-C₆ concentration in the feed mixture on the performance of silicalite-1 membranes was investigated. Three different mixtures of *n*-C₆/2-MP/2,2-DMB with molar ratios of 58.7:21:20.3, 30:33.3:33.7, and 9.7:46:44.3 were used. The molar ratio of 2-MP/2,2-DMB was kept around 1 in all investigated mixtures. Studies performed here show that decreasing the *n*-C₆ concentration in the feed results in a decrease in *n*-C₆ flux through the membrane (see Fig. 12), resulting in a decrease in the permeation fraction of *n*-C₆.

Selectivities of *n*-C₆/2-MP and *n*-C₆/2,2-DMB in the ternary mixture of *n*-C₆/2-MP/2,2-DMB are shown in Fig. 13. These results prove that selectivity is a strong function of the mixture composition; the selectivity decreased along with decreasing *n*-C₆ concentration in the feed. It is known that there is a preference for the adsorption of

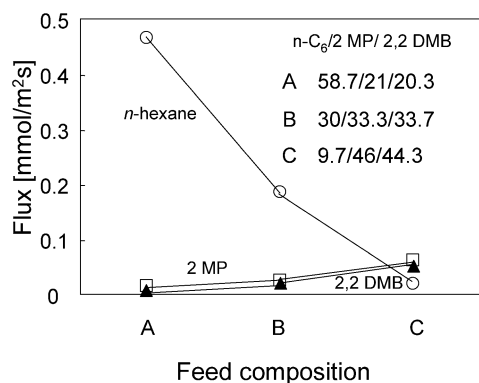


Fig. 12. Fluxes through a silicalite-1 membrane as a function of feed composition in *n*-C₆/2-MP/2,2-DMB mixture permeation at 393 K.

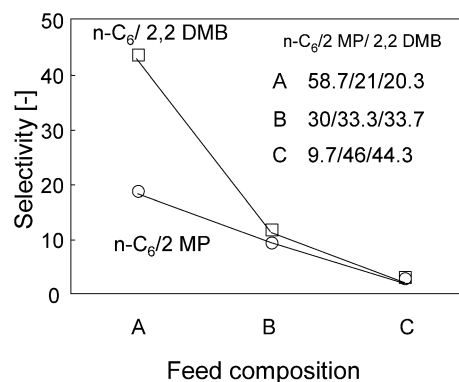


Fig. 13. Separation selectivities for *n*-C₆/2-MP/2,2-DMB mixture component through a silicalite-1 membrane as a function of the feed composition at 393 K.

n-C₆ over 2-MP or 2,2-DMB. The *n*-C₆ can reside anywhere in the pore system, whereas the branched alkane is preferentially adsorbed in the intersections between straight and zigzag channels. The relatively fast permeation of *n*-C₆ is strongly influenced by the presence of the slowly diffusing 2-MP and 2,2-DMB. Most likely this is due to the blocking of the channel intersections by the slowly moving branched alkanes. With decreased *n*-C₆ loading and at the same time increased 2-MP and 2,2-DMB loading, more intersections in the zeolite are blocked, resulting in decreased selectivity of *n*-C₆ over 2-MP or 2,2-DMB. However, a configurational entropy effect can be exploited to obtain high sorption selectivities in the separation of linear from branched alkanes over silicalite-1 membrane [32]. High selectivities with feeds containing a low amount of linear hydrocarbons are envisaged under high upstream pressure. Because of high membrane occupancy operation the pervaporation mode should be considered. However, operation conditions should be optimized to enhance the mobility of permeating molecules inside the zeolite pore network.

Real C₆ hydroisomerization feeds are complex mixtures (see Table 8). The normal/branched hydrocarbon ratios in all of these feeds are around 1. With an optimal configuration, it is expected that normal/branched separation would be accomplished through enhanced process performance.

Purification of the feed is needed since the catalyst is sensitive to poisoning, especially by water. Usually the feed must be desulfurized and dried by contact with molecular sieves. The presence of sulfur decreases the activity of the catalyst, which, may be recovered, however, by the resumption of operation with clean feed. The poisoning produced by the presence of water is irreversible. As stated earlier, small amounts of water can significantly shorten the life of the catalyst. We carried out all of the experiments performed here by feeding the reactor with pure hydrocarbon mixtures. However, it is envisaged that the zeolite membrane will protect the catalyst from feed contaminants (H₂O, S components) in a manner similar to that for coated catalyst particles [36]. Because of the hydrophobic nature of MFI membrane, water should be rejected, protecting the catalyst.

Table 8
Typical feed mixture compositions for C₅–C₆ hydroisomerization reaction

	Akzo Noble [33]	Sie [34]	Hennico [35]
C ₄ components	0.8	0.7	2.8
Pentane	19.3	44.6	23
Iso-pentane	7.8	29.3	16
Hexane	21.1	6.7	23.4
2,2-DMB	0.5	0.6	0.4
2,3-DMB	2.8	1.8	1.8
2-MP	15.9		13
3-MP	12.5	13.9	6.9
Cyclopentane	1.5		1.6
Cyclohexane	4.2	2.4	2.1
Methyl-cyclopentane	9.1	–	5.1
C ₇ + components	2.7	–	2.1
Benzene	1.8	–	1.8

Furthermore, selective rejection of benzene on the membrane could also minimize poisoning of the catalyst [37]. It has been recognized that the presence of benzene in the paraffin feed to the isomerization reactor is detrimental since the benzene is hydrogenated over the isomerization catalyst, causing an increase in reactor temperature, which promotes unwanted cracking reactions and increases hydrogen consumption.

4. Conclusions

A tubular silicalite-1 membrane with a surface area of ca. 30 cm² was prepared by a double-synthesis approach. High quality of the membrane was achieved by high nucleation rates enhanced by a low crystallization temperature in the first synthesis followed by high crystal growth in the second synthesis at high crystallization temperature. The membrane selectively separates linear hydrocarbons from branched ones. It offers interesting prospects for the development of new technologies in the petrochemical industry. The combination of separation and reaction in hydroisomerization of *n*-hexane with a reactor composed of a tubular silicalite-1 membrane packed with Pt-loaded chlorinated alumina catalyst was discussed here. The overall performance of the membrane reactor depends on the effectiveness of the silicalite-1 membrane in removing linear molecules from the feed and, therefore, in delivering *n*-hexane to the reaction zone and then converting it at equilibrium level to isomers. The results from “single-passage mode” show that the system (catalyst and membrane work under the same conditions) has potential for upgrading low-octane hydroisomerization feed streams. *n*-Hexane with a purity of ~ 99% (1% 2-MP, selectivity 24) was supplied selectively through silicalite-1 membrane to the catalyst, where it was 100% selectively hydroisomerized. Silicalite-1 membrane also protects the catalyst against poisoning by impurities (H₂O, benzene). With decreasing membrane thickness, increasing linear hydrocarbon fluxes can be expected. It is

preferable that all linear components from the feed be separated on a silicalite-1 membrane and isomerized. To accomplish complete *n*-hexane separation from the feed, a selective, high-flux membrane is essential. The results indicate the advantages of this type of structured reactor and the prospects for its application.

Acknowledgments

Discussions with Dr. M.L. Maloney, Dr. T.Q. Gardner, and Prof. F. Kapteijn of the Delft University of Technology (TUD) are gratefully acknowledged. Akzo Nobel is acknowledged for supplying the AT-2G catalyst.

References

- [1] T.G. Kaufmann, A. Kaldor, G.F. Stuntz, M.C. Kerby, L.L. Ansell, *Catal. Today* 62 (2000) 77.
- [2] N. Nishiyama, L. Gora, V. Teplyakov, F. Kapteijn, J.A. Moulijn, *Sep. Purif. Technol.* 22–23 (2001) 295.
- [3] R. Krishna, S.T. Sie, *Chem. Eng. Sci.* 49 (1994) 4029.
- [4] L. Trusov, *Membrane Technology* 128 (2000) 10.
- [5] L. Gora, J.C. Jansen, F. Kapteijn, Th. Maschmeyer, in: *International Workshop on Zeolitic and Microporous Membranes, IWZMM2001*, Purmerend, The Netherlands, July 1–4, 2001, p. 89.
- [6] L. Gora, J.C. Jansen, Th. Maschmeyer, *Chem. Eur. J.* 6 (2000) 2537.
- [7] M. Matsukata, E. Kikuchi, *Bull. Chem. Soc. Jpn.* 70 (1997) 2341.
- [8] M.C. Lovallo, A. Gouzinis, M. Tsapatsis, *AIChE J.* 44 (1998) 1903.
- [9] R. Lai, G.R. Gavalas, *Ind. Eng. Chem. Res.* 37 (1998) 4275.
- [10] G. Clet, L. Gora, N. Nishiyama, J.C. Jansen, H. van Bekkum, Th. Maschmeyer, *Chem. Commun.* 1 (2001) 41.
- [11] G. Xomeritakis, S. Nair, M. Tsapatsis, *Micropor. Mesopor. Mater.* 38 (2000) 61.
- [12] T.A.M. Twomey, M. Mackay, H.P.C.E. Kuipers, R.W. Thompson, *Zeolites* 14 (1994) 162.
- [13] L. Gora, K. Streltzyk, R.W. Thompson, D.J. Phillis, *Zeolites* 18 (1997) 119.
- [14] M. Noack, P. Kolsch, R. Schafer, P. Toussaint, I. Siwber, J. Caro, *Micropor. Mesopor. Mater.* 49 (2001) 25.
- [15] Y. Li, X. Zhang, J. Wang, *Sep. Purif. Technol.* 25 (2001) 459.
- [16] J. Hedlund, J. Sterte, M. Anthonis, A.-J. Bons, B. Carstensen, N. Corcoran, D. Cox, H. Deckman, W. de Gijnst, P.-P. de Moor, F. Lai, J. McHenry, W. Mortier, J. Reinoso, J. Peters, *Micropor. Mesopor. Mater.* 52 (2002) 179.
- [17] K. Keizer, A.J. Burggraaf, Z.A.E.P. Vroon, H. Verweij, *J. Membr. Sci.* 147 (1998) 159.
- [18] L. Gora, N. Nishiyama, J.C. Jansen, F. Kapteijn, Th. Maschmeyer, *Sep. Purif. Technol.* 22–23 (2001) 223.
- [19] S. Alfaro, M. Arruebo, J. Coronas, M. Menendez, J. Santamaria, *Micropor. Mesopor. Mater.* 50 (2001) 195.
- [20] J.M. van de Graaf, F. Kapteijn, J.A. Moulijn, *J. Membr. Sci.* 144 (1998) 87.
- [21] R. Krishna, B. Smit, T.J.H. Vlucht, *J. Phys. Chem. A* 102 (1998) 7727.
- [22] W. Zhu, F. Kapteijn, J.A. Moulijn, *Sep. Purif. Technol.* 32 (2003) 223.
- [23] C.L. Flanders, V.A. Tuan, R.D. Noble, J.L. Falconer, *J. Membr. Sci.* 176 (2000) 43.
- [24] D. Schuring, A.O. Koriabkina, A.M. de Jong, B. Smit, R.A. van Santen, *J. Phys. Chem. B* 105 (2001) 7690.
- [25] H. Funke, A.M. Argo, J.L. Falconer, R.D. Noble, *Ind. Eng. Chem. Res.* 36 (1997) 137.
- [26] T. Matsufuji, K. Watanabe, N. Nishiyama, Y. Egashira, M. Matsukata, K. Ueyama, *Ind. Eng. Chem. Res.* 39 (2000) 2434.

- [27] Ch.J. Gump, R.D. Noble, J.L. Falconer, *Ind. Eng. Chem. Res.* 38 (1999) 2775.
- [28] J. Coronas, R.D. Noble, J.L. Falconer, *Ind. Eng. Chem. Res.* 37 (1998) 166.
- [29] B. Millot, A. Methivier, H. Jobic, H. Moueddeb, J.A. Dalmon, *Micropor. Mesopor. Mater.* 38 (2000) 85.
- [30] T. Yashima, Z.B. Wang, A. Kamo, T. Yoneda, T. Komatsu, *Catal. Today* 29 (1996) 279.
- [31] K.-J. Chao, H.-C. Wu, L.-J. Leu, *Appl. Catal. A* 143 (1996) 223.
- [32] R. Krishna, B. Smit, *Chem. Innovation* 31 (1) (2001) 27.
- [33] <http://www.akzonobel-catalysts.com/navigation/isomerization/home.htm>.
- [34] G. Ertl, H. Knozinger, J. Weitkamp, in: *Handbook of Heterogeneous Catalysis*, vol. IV, VCH, Weinheim, 1997, p. 2012.
- [35] A. Hennico, J.-P. Cariou, *Hydrocarbon Processing*, November (1999) 68.
- [36] N. Nishiyama, K. Ichioka, D.-H. Park, Y. Egashira, K. Ueyama, L. Gora, W. Zhu, F. Kapteijn, J. Moulijn, *Ind. Eng. Chem. Res.* 43 (2004) 1211.
- [37] A.P. Voss, M.J. Pedersen, US Patent 5 770 781 (1998), to Atlantic Richfield Co.